IRAQI JOURNAL OF APPLIED PHYSICS
Vol. 22, No. 2, April-June 2026, pp. 317-321

Influence of Argon Gas Flow Rate on Properties and Coupling Behavior of Iron Plasma

Muna A. Issa

Quality Assurance and Performance Evaluation Department, Mustansiriyah University, Baghdad, IRAQ
Corresponding author email: muna.ahmed@uomustansiriyah.edu.iq

Optical Emission Spectroscopy (OES) was used to study the features of Fe plasma according to the Ar gas flow rate. With increasing gas flow rate from 1.0 to 2.0 L/min, the electron temperature increased from 0.369 to 0.480 eV, and the electron density increased from 12.162 ± 0.58 ×1017 to 13.851±0.67 ×1017 cm^{-3}. There was also an increase in plasma frequency (9.90×10^{12} to 10.57×10^{12} Hz) and a slight increase in Debye length ($4.091\pm0.32\times10^{-6}$ to $4.373\pm0.37\times10^{-6}$ cm). These trends suggest that increased flow rates promote a higher degree of excitation and steadiness, producing stronger supporting gas (N_2 and Ar) and Fe I emission lines. In addition, an analysis of the behavior of the coupling parameter (Γ) indicates that plasma remains near ideal with Γ = 0.671±0.19, 0.561±0.08, and 0.539±0.08 with the average inter-particle distance of 5.8116±0.41, 5.6111±0.37, and 5.5651±0.39 nm, respectively. As the Ar flow rate increases, Γ decreases, indicating that under higher gas flow conditions, the plasma is closer to an ideal state and less strongly coupled.

Keyword: Iron plasma; Argon gas flow; Optical Emission spectroscopy (OES); Coupling parameter
Received: 31 August 2025; Revised: 28 October; Accepted: 4 November 2025; Published: 1 April 2026

1. Introduction

Plasma, the fourth state of matter, is a very complex medium that consists of electrons, ions, and neutral particles [1]. Owing to its physical properties, plasma has been used as one of the core components of several applications in modern-day technology, which include metallurgy, nuclear physics, surface treatment, thin-film deposition, and medical and environmental technology [2,3]. On the other hand, plasma parameters such as electron temperature (T_e), electron density (n_e), Debye length (λ_D), plasma frequency (f_p), etc., are fundamental to investigate for determining the efficiency and stability of plasma-based processes [4]. The Ar gas flow rate is an essential parameter affecting the discharge behavior, since it controls the concentration of the reactive species in the plasma column where they are subject to ionization, collision, and energy transfer processes [5]. As a result, gas flow is one of the easiest ways to tune plasma [6]. Due to its use in applications accumulated in structures of many industrial and scientific fields, as well as its function in energy from iron alloys, magnetic materials, and energy storage systems [7]. Fe-based plasma can indeed help us to understand processes like melting and/or deposition, and/or surface modification, and also pave the way for new materials.

The coupling parameter of the plasma (Γ) is an important indicator of plasma behavior: in combination with some intrinsic plasma parameters, it can be used to classify plasma as quasi-ideal, weakly non-ideal, or strongly coupled. The interaction parameter, Γ, indicates the relative strength of Coulomb interactions to thermal motion and can reveal information about microscopic dynamics at work in the plasma, as well as stability and usability information under various operating conditions [8]. However, the influence of Ar gas flow rate on Γ of Fe-based plasma jets at atmospheric pressures is not studied in the literature despite its importance. An investigation of the behavior of Γ as a function of Ar gas flow rate could provide greater insights into plasma behavior than conventional diagnostics like temperature and density. This analysis would allow for the optimization of operational parameters to achieve physical parameters that are required for various Fe-based plasma applications.

2. Experimental Method

A diagram of the plasma jet system used in this study is presented in Fig. (1). The experimental setup is composed of a cold atmospheric plasma jet system, an Fe electrode, argon (Ar) gas, a voltage controller, and a high-voltage DC power supply. The plasma jet is generated by a 14 kV, 40 kHz power supply with open circuit protection under ambient atmospheric conditions. Ar gas is introduced through a needle cathode connected to the power supply. The anode is a 5×10 cm Fe strip (2 cm^2 immersion area in water).

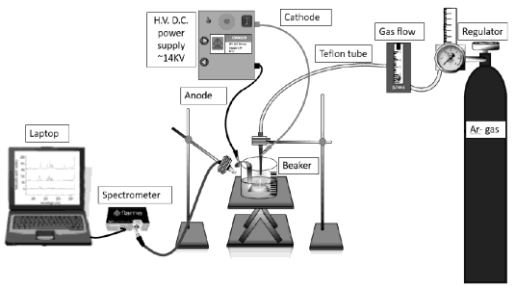

Fig. (1) Optical emission spectroscopy diagnostic and plasma jet system configuration

Emission lines of Fe I primarily arise from the physical sputtering of the Fe anode by energetic Ar ions

 © ALL RIGHTS RESERVED

and metastable species. These interactions release neutral Fe atoms into the plasma that are subsequently excited and emit characteristic emission lines. Despite the occurrence of a small degree of electrochemical dissolution of Fe due to anodic bias in the plasma-liquid configuration, this is negligible due to the high voltage, short discharge times, lack of a strong electrolyte at the interface, and fast bombardment of ions; consequently, sputtering is the key mechanism by which Fe is introduced into the plasma. A stable plasma jet is created when Ar gas is passed through the needle, which itself is positioned 2 mm above the surface of the water.

Nanoparticle formation was monitored by optical emission spectroscopy and used to record the plasma behaviour based on the Ar gas flow rate (1, 1.5, and 2 L/min); specifically, the identification of the excited species and their relative densities in the discharge region was assessed by analyzing the plasma jet configuration. The spectrometer integration time was 2 s. Plasma emissions were collected by positioning a quartz optical fiber near the plasma plume (~8 cm) and tilted (45°) with respect to the jet axis to improve the signal. Measurements were performed under atmospheric conditions in a plasma–liquid configuration, where the discharge impinged upon the water surface. Both radial and axial spectra were recorded; the axial spectra were used to calculate electron temperature and density by assuming spatial homogeneity in the plasma within the optical collection volume. Spectral data were recorded using an S3000 UV and near-infrared spectrometer between 250 and 1000 nm in the radial and axial directions. The elemental composition, as well as several quantitative and qualitative parameters (e.g., electron density and electron temperature), can be determined from the shape, width, and distribution of the spectral signals.

The plasma temperature is associated with several plasma attributes, including the distribution of energy level populations and particle speeds. A Boltzmann plot was employed to determine the electron temperature of the plasma, assuming local thermodynamic equilibrium [9]:

$$ln\left[\frac{\lambda_{ji} I_{ji}}{hcA_{ji}g_j}\right] = -\frac{1}{kT}(E_j) + ln\left|\frac{N}{U(T)}\right|, \quad (1)$$

where λ_{ji} denotes the wavelength of the emission peak, N indicates the number density, $U(T)$ represents the partition function, $h\upsilon_{ji}$ is the photon energy of the transition, E_j is the excitation energy of the level, k_B denotes the Boltzmann constant, and T_e indicates the electron temperature

Electron density is the number of free electrons per unit volume of plasma. It can be quantified with techniques like Thomson scattering, microwave spectroscopy, and plasma spectroscopy. This study infers electron density from the linear Stark broadening of spectral peaks. Local electric fields further distort the atomic spectra via what is called Stark broadening, which corresponds to the interaction of the plasma with the surrounding charged particles. Of all processes from the spectrum lines, the Stark broadening is an utterly severe phenomenon, and it is necessary in order to measure electron density for certain electron temperature conditions. The electron density can be calculated using Eq. (2) [9]:

$$n_e\,(cm^{-3}) = (2w_s\Delta\lambda)\,N_r, \quad (2)$$

where ω_s is the Stark broadening coefficient of the Ar I 763.51 nm emission line [10]; this is equal to 0.074 nm under standard laboratory conditions

The 763.51 nm Ar line was selected for the electron density calculations; at this wavelength, a strong peak with relatively non-overlapping transitions exists, and thus, the broadening of the peak due to Stark broadening can be decoupled from other broadening mechanisms (e.g., the Doppler and van der Waals effects) [6]. As a result, this line is a stable diagnostic signature of an argon plasma in the atmosphere. N_r is the reference electron number density; this is generally considered to be a constant in practical plasma diagnostics. Eq. (2) is the linear approximation of Stark broadening theory, which is approximately valid in the normal range of electron densities and temperatures of low-temperature plasmas. The obtained electron temperatures were fairly consistent in digits, in eV and K when converted (T ≈ 4000-5600 K), confirming the applicability of this diagnostic for plasma parameters. $\Delta\lambda$ represents the broadening of the emission line in nm.

The frequency of plasma is entirely dependent on density and is a key characteristic of plasmas. Plasma generally has a high frequency because electrons have a very low mass. Plasma frequency can be determined from the following formula [11]:

$$f_p\,(Hz) = 8.98\sqrt{n_e} \quad (3)$$

Debye shielding (λ_D) maintains the quasi-neutrality of plasma by reducing the influence of the electric field on local fields. The equation for the Debye length (λ_D) is as follows [11]:

$$\lambda_D\,(cm) = 743\sqrt{\frac{T_e}{n_e}} \quad (4)$$

Finally, the plasma coupling parameter (Γ) was calculated by [12]:

$$\Gamma = \frac{e^2}{4\pi\,\varepsilon_o a k_B T_e} \quad (5)$$

where e is the charge of an electron (1.602×10^{-19} C), ε_0 is the permittivity of free space (8.85×10^{-12} F/m), a is the average inter-particle distance (nm), and k_B is the Boltzmann constant (1.380×10^{-23} J/K)

For practical calculations, where T_e is expressed in eV and a in nm, the above equation can be simplified to:

$$\Gamma = \frac{1.43996}{a\,T_e} \quad (6)$$

The average inter-particle distance was obtained using the measured electron density according to Eq. (7) [12]:

$$a = \left(\frac{3}{4\pi n_e}\right)^{1/3} \quad (7)$$

 © ALL RIGHTS RESERVED

If $\Gamma << 1$, the plasma is ideal; if $\Gamma < 1$, the plasma is weakly non-ideal, and if $\Gamma > 1$, the plasma is strongly coupled [12].

3. Results and Discussion

Figure (2) displays the data over the spectral range of 250 to 1000 nm, including the molecular transitions of N_2 and N_2^+, and the characteristic peaks of OH and NO. The source of these molecular emissions is the entrainment of ambient atmosphere into the Ar plasma jet. Once the jet travels through ambient air, the discharge region is seeded with N, O, and water vapor, which are ionized and excited by fast electrons, and subsequently, Fe atoms are sputtered and excited. Ar emission lines (Ar I) were also observed in this range (between 700 and 900 nm), and their intensity was considerably enhanced by higher gas flow rates. Characteristic Fe I lines between 200 and 300 nm (217.81, 248.81, and 271.90 nm) as shown in Fig. (3). This gradual line enhancement occurs with flow rates. These results indicate that high flow rates of the supporting gas (N_2 and Ar) and Fe emission lines become more intense with increasing gas flows as the excitation conditions and plasma are more stable, and this is consistent with [13].

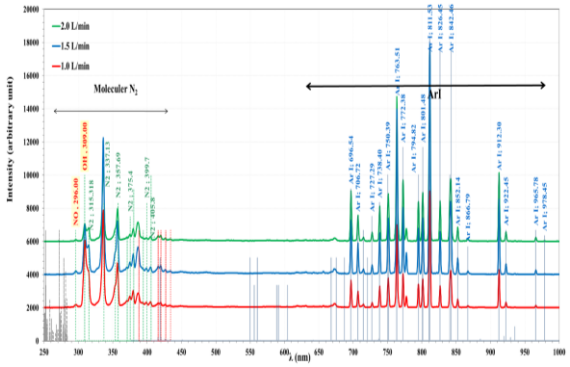

Fig. (2) Plasma emission spectra of argon gas flow rate

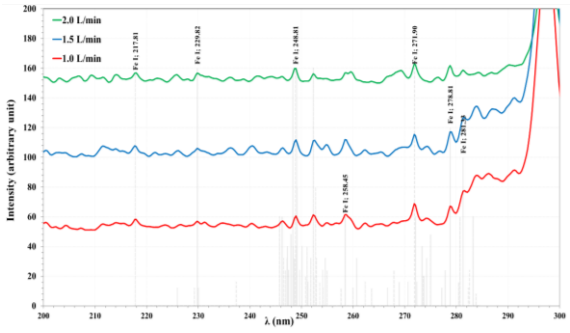

Fig. (3) Plasma emission spectra of iron by argon gas flow rate

Figure (4) shows the Boltzmann plots of the plasma jet at flow rates of 1.0, 1.5, and 2.0 L/min. Across the board, we see a distinct linear trend, thus validating the method for using this peak to calculate the electron temperature of the plasma. To obtain accurate temperature measurements, we built the Boltzmann plots with many isolated Ar I emission lines at 696.5, 706.9, 763.9, 801.4, and 811.5 nm. The results showed an increase in the gradient of the plots with the flow rate, suggesting a minor increase in the electron temperatures. That relates to the spectral finding, where we see more excitation and ionization occurring in Fe-based plasma at higher flow rates. The enhanced performance can be attributed to improved plasma confinement and higher reduced electric field (E/N), leading to faster electron heating, along with reductions of charged and excited particle losses by diffusion from the plasma core [14].

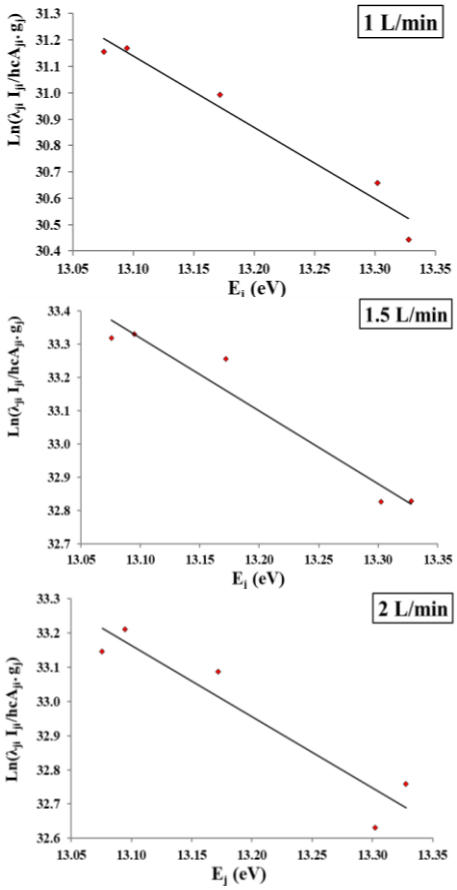

Fig. (4) Linear fitting of Boltzmann plots for ArI lines by gas flow rate

Electron density was calculated for the studied flow rates through the Lorentzian fitting of selected emission lines (Fig. 5). The line broadening obtained from this method was strongly consistent with the spectral profiles as demonstrated by the fitting curves. Both the intensity and line width increased with flow rate, which in turn corresponds to increased electron density in the plasma. These results are consistent with previous plasma parameter analyses.

 © ALL RIGHTS RESERVED

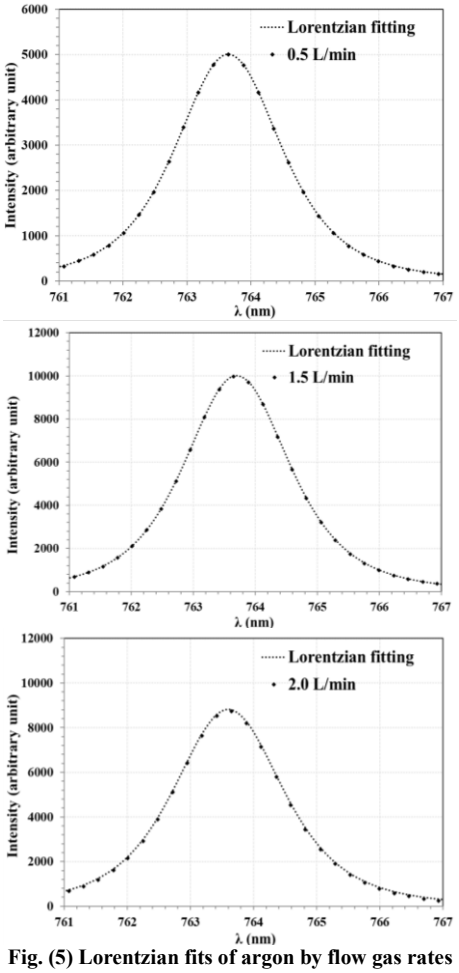

Fig. (5) Lorentzian fits of argon by flow gas rates

Figure (6) presents the relationship between electron density and temperature with Ar gas flow rate. At higher flow rates, there is a clear increasing trend between these parameters. Specifically, electron density (n_e) increases from 12.162±0.58 $\times 10^{17}$ cm^{-3} at 1.0 L/min to 13.851±0.67 $\times 10^{17}$ cm^{-3} at 2.0 L/min, while electron temperature (T_e) increases from 0.480±0.11 eV to 0.369±0.05 eV across the same range. This result is consistent with previous work [15], indicating that ionization is more efficient and energy transfer processes are more effective at higher flow rates, as reflected in the increased electron density and temperature of the plasma. These results are consistent with observed spectra and line broadening analysis, indicating that the Ar flow rate is a key factor that controls the energetic behavior of Fe-based plasma.

Higher flow rates also correspond to increasing electron temperatures, line profile widths, electron densities, and plasma frequencies; it is also associated with a small rise in the Debye length (table 1). These results are consistent with previous work [16]. A statistical analysis of the measured plasma parameters, including T_e, FWHM, n_e, f_p, λ_D, a, and Γ is summarized in table (1). Notably, electron density increased significantly from 12.162±0.58 $\times 10^{17}$ to 13.851±0.67 $\times 10^{17}$ cm^{-3} as the Ar gas flow rate increased from 1.0 to 2.0 L/min (p = 0.0374). A similarly large increase in plasma frequency was also noted (p = 0.0450). However, the differences in T_e, FWHM, and λ_D were not statistically significant (p > 0.05; Table 3). There was also a statistically significant decrease in the coupling parameter from 0.671±0.19 to 0.539±0.08 with increasing flow rate (p = 0.0439), indicating that the plasma is weakly coupled (Γ < 1); i.e., the electron thermal energy dominates over Coulomb interactions. Table (1) shows that the individual Γ values were closely related to the average inter-particle distances 5.8116±0.41 nm, 5.6111±0.37 nm, and 5.5651±0.39 nm, at flow rates of 1.0, 1.5, and 2.0 L/min, respectively. This is representative of reproducible and controllable discharge in atmospheric Ar jets, which is necessary for consistent nanoparticle generation and plasma–liquid interaction applications.

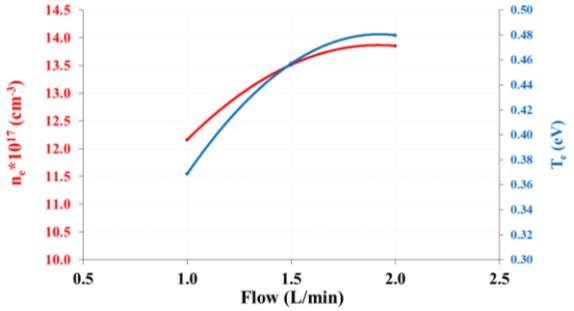

Fig. (6) Change in electron temperature T_e and electron density n_e of iron plasma by flow rate

4. Conclusions

The results show that the Ar gas flow rate is a key factor that can be manipulated to control the characteristics of Fe-based plasma. Higher flow rates result in increasing electron temperature, electron density, plasma frequency, and line broadening, supporting efficient excitation and stable plasma expansion. The measured coupling parameter values (Γ = 0.671±0.19, 0.561±0.08, and 0.539±0.08 for gas flow rates between 1.0 and 2.0 L/min; supported by inter-particle distance) indicate that the plasma is weakly coupled (Γ < 1). The reduction in Γ with increasing Ar gas flow rate indicates that increased flow rates produce a more ideal plasma with reduced coupling. These findings demonstrate that tuning the Ar gas flow can help obtain stable, near-ideal plasma conditions that are suitable for advanced physical and industrial applications.

References

[1] M.A. Issa and K.A. Aadim, "Study the structural and optical properties of zinc oxide prepared by pulse laser deposition", *J. Opt.*, 1(1) (2024) 1-6.

[2] H. Takabe, "Basic properties of plasma in fluid model", in **The Physics of Laser Plasmas and**

 © ALL RIGHTS RESERVED

Applications – vol. 2: Fluid Models and Atomic Physics of Plasmas, Springer (2024), pp. 15-97.

[3] M.A. Issa and K.A. Aadim, "Optical and structural characterization of ZnO:NiO nanocomposite prepared by pulsed laser deposition method", *J. Opt.*, 1(1) (2024) 1-6.

[4] M.A. Issa and K.A. Aadim, "Influence of laser energy on structural and optical properties of $ZnO_{(x)}$:$NiO_{(1-x)}$ films prepared by pulsed laser deposition", *J. Opt.*, 1(1) (2024) 1-7.

[5] G. Tetard et al., "Discharge dynamics, plasma kinetics and gas flow effect in argon–acetylene discharges", *Plasma Sources Sci. Technol.*, 30(10) (2021) 105015.

[6] Q. Al-Obaidi et al., "A comprehensive analysis of the hydrogen generation technology through electrochemical water and industrial wastewater electrolysis", *Pol. J. Chem. Technol.*, 26(3) (2024) 39-50.

[7] S. Santosh and M. Pavithran, "Iron-based smart alloys for critical applications: a review on processing, properties, phase transformations, and current trends", *J. Mater. Sci.: Mater. Eng.*, 19(1) (2024) 8.

[8] B. Santos, "The effects of interparticle potentials on nanoparticle coagulation in low-temperature plasmas", Ph.D. dissert., Institut National de la Recherche Scientifique (Canada) (2020).

[9] S.A. Mutar, I.K. Abbas and K.A. Aadim, "Effect of applied voltage on spectroscopic characterization of neon plasma", *Iraqi J. Sci.*, 65(8) (2024) 4740-4747.

[10] H.R. Griem, **"Spectral Line Broadening by Plasmas"**, Academic Press (NY, 1974).

[11] M.A. Issa and K.A. Aadim, "Optical emission spectroscopy of zinc oxide doped nickel oxide to calculate plasma parameters using the Boltzmann plot method", *Iraqi J. Phys.*, 23(2) (2025) 118-127.

[12] J. Clérouin et al., "Behavior of the coupling parameter under isochoric heating in a high-Z plasma", *Phys. Rev. E*, 87(6) (2013) 061101.

[13] A.J. Mohamed, M.K. Khalaf and A.S. Jasim, "The study of the characteristics of a microwave plasma jet operated with Ar at atmospheric pressure", *Tikrit J. Pure Sci.*, 27(4) (2022) 70-76.

[14] U.R. Kortshagen et al., "Nonthermal plasma synthesis of nanocrystals: fundamental principles, materials, and applications", *Chem. Rev.*, 116(18) (2016) 11061-11127.

[15] B.A.Z.Z.M. Abood and A.A. Khadayeir, "Measurement of electron temperature (Te) and electron density (ne) in cold plasma jets using optical emission spectroscopy (OES) method", *Mustansiriyah J. Pure Appl. Sci.*, 2(2) (2024) 126-133.

[16] R.A.S. Alkareem et al., "Plasma parameters diagnosis of laboratory Ar/O_2 cold atmospheric plasma jet using different potential discharges", *Al-Mustansiriyah J. Sci.*, 34(3) (2023) 124-131.

[17] Statistical Packages of Social Sciences-SPSS/IBM Statistics 26 step by step, 16th ed. (2019), https://doi.org/10.4324/9780429056765.

Table (1) Variation of plasma parameters with gas flow rate

Gas flow (L/min)	Means ± SE						
	T_e (eV)	FWHM (nm)	n_e x10^{17} (cm^{-3})	f_p*10^{12} (Hz)	λ_D x10^{-6} (cm)	a (nm)	Γ
1 L/min	0.369 ± 0.05	1.800 ± 0.11	12.162 ± 0.58 b	9.903 ± 0.48	4.091 ± 0.32	5.8116 ± 0.41	0.671 ± 0.19 a
1.5 L/min	0.457 ± 0.08	2.000 ± 0.17	13.514 ± 0.61 a	10.439 ± 0.55	4.321 ± 0.29	5.6111 ± 0.37	0.561 ± 0.08 b
2.0 L/min	0.480 ± 0.11	2.050 ± 0.24	13.851 ± 0.67 a	10.569 ± 0.61	4.373 ± 0.37	5.5651 ± 0.39	0.539 ± 0.08 c
L.S.D	0.141 NS	0.238 NS	1.063*	0.4288*	0.5117 NS	0.391 NS	0.127*
P-value	0.1749	0.092	0.0374	0.04502	0.3679	0.2581	0.0439

Means with the different letters in the same column differed significantly.
*($p \leq 0.05$); NS: non-significant [17].

 © ALL RIGHTS RESERVED